

Aquaporin-6: An intracellular vesicle water channel protein in renal epithelia

MASATO YASUI*[†], TAE-HWAN KWON^{†‡}, MARK A. KNEPPER[§], SØREN NIELSEN^{‡¶}, AND PETER AGRE*[¶]

*Departments of Biological Chemistry and Medicine, Johns Hopkins University School of Medicine, Baltimore, MD 21205-2185; [‡]Department of Cell Biology, University of Aarhus, DK 8000, Aarhus C, Denmark; and [§]Laboratory of Kidney and Electrolyte Metabolism, National Heart, Lung and Blood Institute, National Institutes of Health, Bethesda, MD 20892

Communicated by Gerhard Giebisch, Yale University School of Medicine, New Haven, CT, February 9, 1999 (received for review November 18, 1998)

ABSTRACT All characterized mammalian aquaporins (AQPs) are localized to plasma membranes where they function chiefly to mediate water transport across cells. Here we show that AQP6 is localized exclusively in intracellular membranes in renal epithelia. By using a polyclonal antibody to the C terminus of AQP6, immunoblots revealed a major 30-kDa band in membranes from rat renal cortex and medulla. Endoglycosidase treatment demonstrated presence of an intracellular high mannose glycan on each subunit. Sequential ultracentrifugation of rat kidney homogenates confirmed that AQP6 resides predominantly in vesicular fractions, and immunohistochemical and immunoelectron microscopic studies confirmed that >98% of AQP6 is located in intracellular membrane vesicles. In glomeruli, AQP6 is present in membrane vesicles within podocyte cell bodies and foot processes. In proximal tubules, AQP6 is also abundant in membrane vesicles within the subapical compartment of segment 2 and segment 3 cells, but was not detected in the brush border or basolateral membranes. In collecting duct, AQP6 resides in intracellular membrane vesicles in apical, mid, and basolateral cytoplasm of type A intercalated cells, but was not observed in the plasma membrane. Unlike other members of the AQP family, the unique distribution in intracellular membrane vesicles in multiple types of renal epithelia indicates that AQP6 is not simply involved in transcellular fluid absorption. Moreover, our studies predict that AQP6 participates in distinct physiological functions such as glomerular filtration, tubular endocytosis, and acid-base metabolism.

The aquaporins (AQPs) are a family of water-selective membrane channels found in mammals, invertebrates, plants, and microorganisms where they mediate the entry and release of water from cells (1). AQPs are well-characterized in mammalian kidney where they facilitate transepithelial water absorption (2). AQP1 is present in apical and basolateral membranes of renal proximal tubules and descending limbs of Henle's loop where it confers transcellular water permeability needed for reabsorption of water from filtrate (3–5). AQP2 is expressed in principal cells of collecting duct; in response to vasopressin, AQP2 translocates from intracellular vesicles to the apical plasma membrane, thereby increasing water permeability necessary for the final concentration of urine (6–8). AQP3 and AQP4 reside in the basolateral membranes of collecting duct principal cells, providing the exit pathways to the interstitium (9, 10). Originally identified in testis, AQP7 is permeated by water and glycerol and also is expressed in kidney (11).

Kidney is the model organ for transport physiologists, and existence of still-unidentified AQPs is suspected in renal tissues. A cDNA from rat kidney (WCH3) and the human

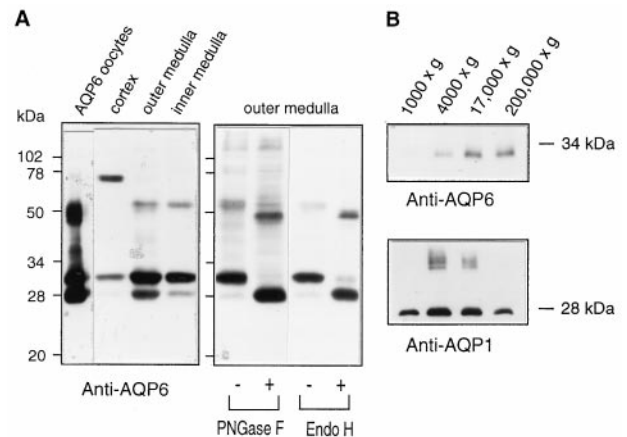


Fig. 1. Immunoblot analyses of tissue expression and N-glycosylation of AQP6. (A, Left) Anti-AQP6 immunoblot of membranes isolated from *X. laevis* oocytes injected with AQP6 cRNA or indicated rat kidney tissues (see *Materials and Methods*). (Right) Anti-AQP6 immunoblot of membrane proteins from outer medulla before (–) or after (+) digestion with peptide/N-glycosidase F (PNGase F) or endoglycosidase Hf (Endo H). (B) Immunoblots of kidney membrane fractions; pellets from sequential centrifugation at 1,000 ×, 4,000 ×, 17,000 ×, and 200,000 × g.

homolog (hKID) slightly increased osmotic water permeability of *Xenopus laevis* oocytes, but unsuccessful attempts to raise antibodies led the authors to conclude that the protein is not immunogenic (12, 13). The International Human Genome Nomenclature Committee adopted the name aquaporin (AQP) as the referencing system (14). AQP6 was designated for rat WCH3 and human hKID (15), although the cellular locations are still not established.

While searching for new AQPs in kidney by PCR, we recently isolated a rat cDNA clone (GenBank accession no. AF083879) encoding a water channel protein (AQP6), which is closely related to rat WCH3 and human hKID. In contrast to previous reports (12, 13), here we note that AQP6 protein is a potent inducer of antibodies in rabbits (Fig. 1). By using classical techniques of light microscopy and immunogold electron microscopy, we have identified AQP6 in unique intracellular sites, predicting that AQP6 is functionally distinct from other known AQPs.

MATERIALS AND METHODS

AQP6 Antibodies. Rabbits were immunized with keyhole limpet hemocyanin conjugated with synthetic peptide (NH₂-

The publication costs of this article were defrayed in part by page charge payment. This article must therefore be hereby marked "advertisement" in accordance with 18 U.S.C. §1734 solely to indicate this fact.

PNAS is available online at www.pnas.org.

Abbreviation: AQP, aquaporin.

Data deposition: The sequence reported in this paper has been deposited in the GenBank database (accession no. AF083879).

[†]M.Y. and T.-H.K. contributed equally to this work.

[¶]To whom reprint requests should be addressed. e-mail: pagre@bs.jhmi.edu or sn@ana.aau.dk.

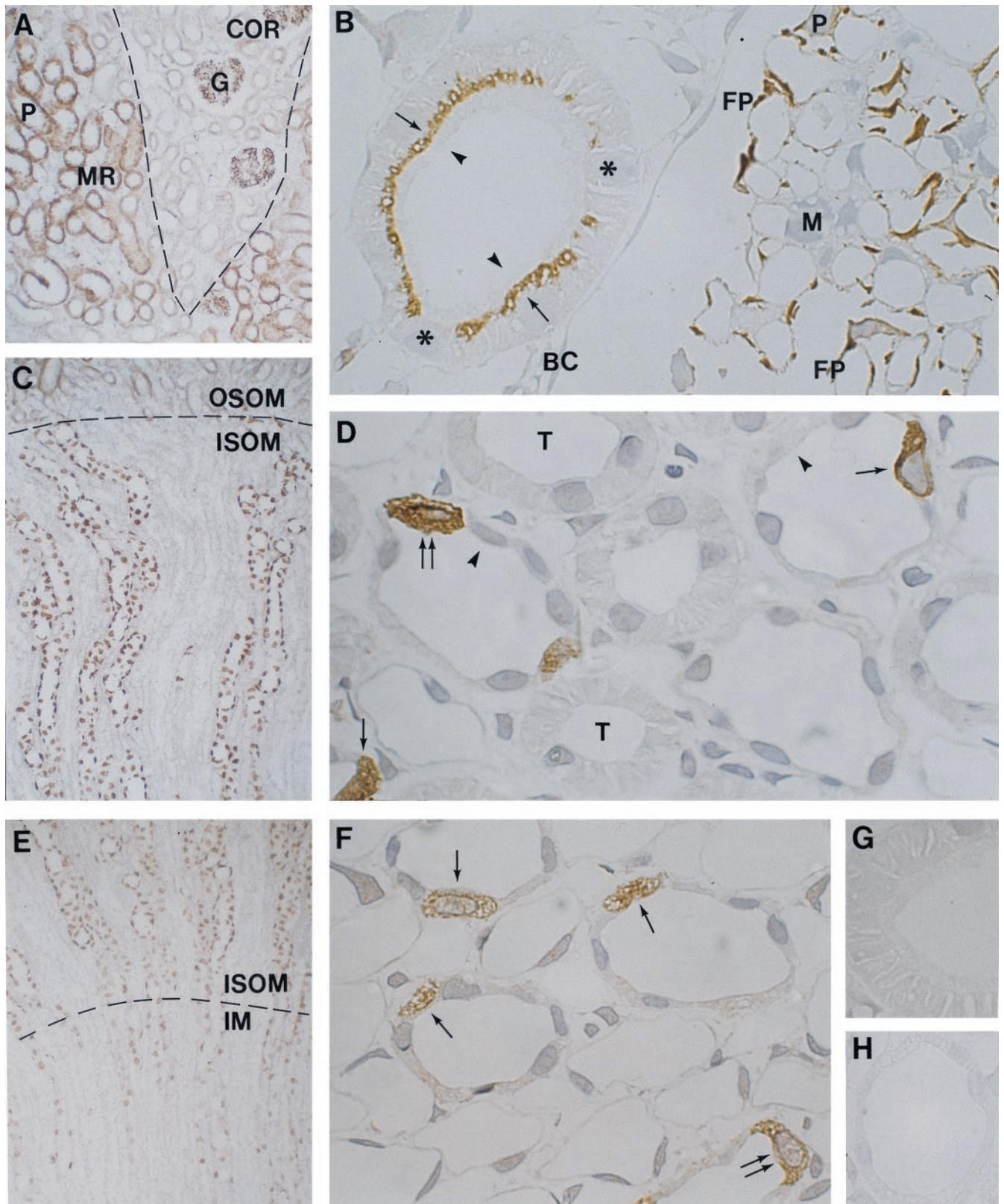


FIG. 2. Immunocytochemical analyses of cellular and subcellular localization of AQP6 in kidney using immunoperoxidase labeling of cryostat (*A, C, and E*) and semithin cryosections (*B, D, and F-H*). (*A*) AQP6 labeling of straight proximal tubules (P) in medullary rays (MR, stippled lines) and glomeruli (G) in cortex (COR). (*B*) AQP6 in subapical domains of proximal tubule cells (arrows) but not in brush border (arrowheads) or basolateral plasma membranes. A sharp transition separates labeled from unlabeled proximal tubule cells (*). AQP6 labeling of podocyte cell bodies (P) and foot processes (FP) but not of Bowman capsule (BC) or mesangial cells (M) of glomerulus. (*C*) Abundant AQP6 labeling of collecting duct in the outer medulla (OSOM, outer stripe; ISOM, inner stripe). (*D*) Abundant AQP6 labeling within type A intercalated cells (arrows). Absent AQP6 labeling in principal cells (arrowheads), thick ascending limbs (T), thin descending limbs, and vascular structures. (*E*) AQP6 within intercalated cells of collecting ducts in the inner stripe of outer medulla and inner medulla (IM). (*F*) AQP6 labeling of cytoplasm in type A intercalated cells (arrows) of inner medullary collecting duct. (*G*) Peptide-absorbed anti-AQP6 immunolabeling control of proximal tubule cells and (*H*) collecting duct cells in inner stripe of outer medulla. Magnifications: $\times 150$ (*A, C, and E*); $\times 1,100$ (*B, D, and F-H*).

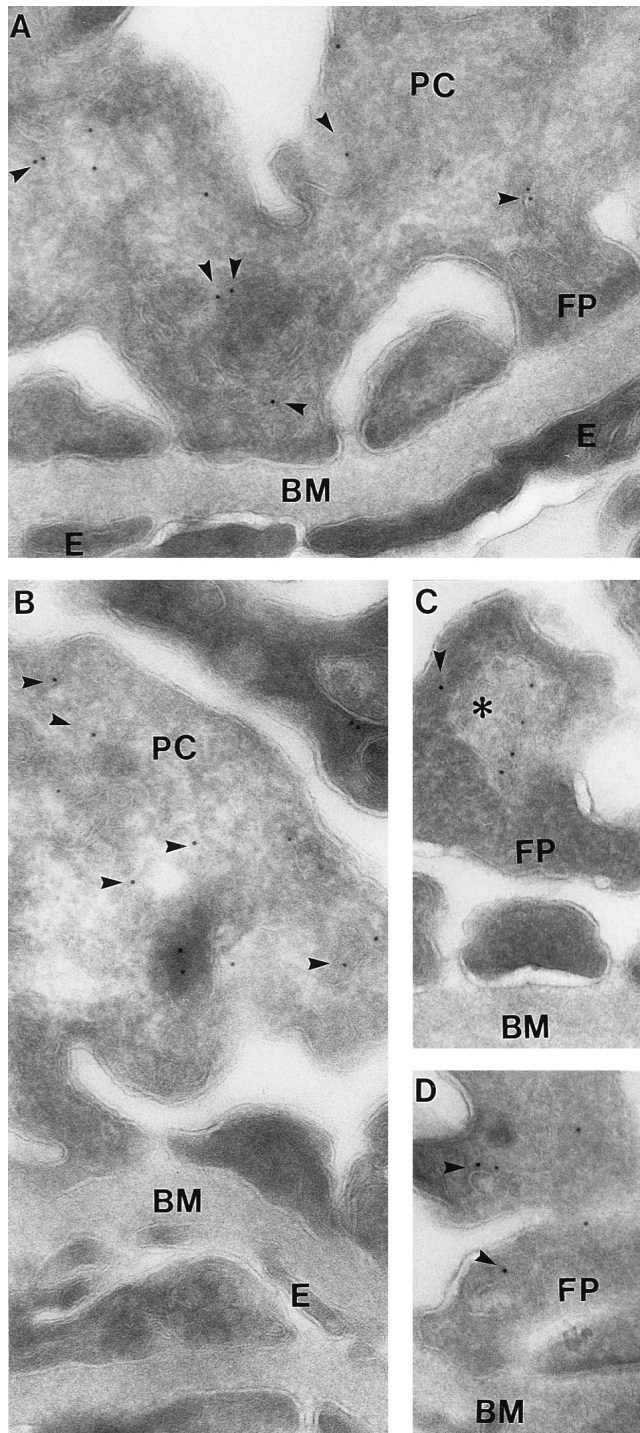


FIG. 3. Immunoelectron microscopy of AQP6 in ultrathin cryosections of glomerulus. Immunogold AQP6 labeling of intracellular structures (arrowheads) in foot processes and cell bodies of podocytes; no labeling of endothelial and mesangial cells (A and B). Some AQP6 labeling associated with larger bodies resembling lysosomes or multivesicular bodies (*, C). BM, basement membrane; E, endothelial cell; FP, foot process; PC, podocyte cell body. Magnification: $\times 60,000$.

CKVEKVVVDLEPQKKESQTNSEDTEV-COOH) corresponding to amino acids 251–274 near the C terminus of AQP6 with an additional N-terminal cysteine. Antisera were screened by immunoblotting with membranes from oocytes injected with AQP6 cRNA. Anti-AQP6 IgG was affinity-purified with a column containing 2.5 mg of the peptide attached by sulfhydryl linkage to maleimide-activated agarose beads (Pierce Immobilization Kit no. 2) as described (9, 10).

Analysis of AQP6 in Membranes. Defolliculated stage V–VI oocytes from *X. laevis* were injected with 50 nl of water or 5 ng of AQP6 cRNA and incubated for 3–4 days (16). Total membranes were isolated from groups of five oocytes or dissected rat kidney cortex, outer medulla, and inner medulla (9, 10). Selected samples were digested with 10 $\mu\text{g}/\text{ml}$ peptide/*N*-glycosidase F or 10 $\mu\text{g}/\text{ml}$ endoglycosidase Hf (New England Biolabs) (17). The preparations were solubilized in 2% SDS, electrophoresed into a 12% SDS-polyacrylamide gel (18), transferred to nitrocellulose, incubated with affinity-purified anti-AQP6 (1.2 $\mu\text{g}/\text{ml}$), and visualized by using ECL chemiluminescence (Amersham Pharmacia). To control for nonspecific reactions, blocking experiments were performed by adding 1 μg of synthetic peptide to the anti-AQP6 blotting solutions (≈ 10 -fold molar excess) and incubated overnight before immunoblotting. To evaluate whether AQP6 resides in plasma membranes or an intracellular microsomal population, renal medulla was homogenized and serially exposed to increasing ultracentrifugation forces (10).

Immunocytochemistry and Immunoelectron Microscopy. Kidneys from normal Munich-Wistar rats or vasopressin-deficient Brattleboro rats were fixed by retrograde perfusion via the aorta with periodate-lysine-paraformaldehyde (0.01 M NaIO_4 , 0.075 M lysine, 2% paraformaldehyde, in 0.0375 M Na_2HPO_4 buffer, pH 6.2). Tissue blocks prepared from cortex, outer and inner stripe of outer medulla, and inner medulla were cryoprotected with 2.3 M sucrose containing 2% paraformaldehyde, mounted on holders, and rapidly frozen in liquid nitrogen (3). For preparation of cryostat sections, tissue was cryoprotected in 30% sucrose (19). Cryostat sections (10–15 μm) and semithin sections (0.8–1 μm , Reichert Ultracut S Cryoultramicrotome) were incubated overnight at 4°C with affinity-purified anti-AQP6 antibody, and labeling was visualized with horseradish peroxidase-conjugated secondary antibody (P448 1:100, Dako).

For immunoelectron microscopy, the frozen samples were either cryosectioned directly for immunogold labeling (3) or freeze-substituted in a Reichert AFS freeze substitution unit (20). In brief, the samples were sequentially equilibrated over 3 days in methanol containing 0.5% uranyl acetate at temperatures gradually raised from -80°C to -70°C , then rinsed in pure methanol for 24 hr while increasing the temperature from -70°C to -45°C , and infiltrated with Lowicryl HM20 and methanol 1:1, 2:1 and, finally, pure Lowicryl HM20 before UV polymerization for 2 days at -45°C and 2 days at 0°C . Immunolabeling was performed on ultrathin Lowicryl HM20 sections (21), which were incubated with anti-AQP6, and labeling was visualized with goat-anti-rabbit IgG conjugated to 10 nm colloidal gold particles (GAR.EM10, BioCell Laboratories, 1:50). Sections were stained with uranyl acetate and lead citrate before examination in Philips CM100 or Philips 208 electron microscopes.

RESULTS

AQP6 in Cell Membranes. Anti-AQP6 specifically recognizes a major 30-kDa band and a 28-kDa band on immunoblots of membranes from AQP6 oocytes, rat renal cortex, outer medulla, and inner medulla (Fig. 1 *A, Left*). In addition, the renal cortex contained a strong band at approximately 75 kDa, and membranes from AQP6 oocytes and renal medulla contained bands at ≈ 55 kDa. The specificities of these reactions were confirmed by preabsorbing the anti-AQP6 with a molar excess of the immunizing peptide (not shown). No reactions were detected in membranes from oocytes injected with 50 nl of water (not shown).

The deduced amino acid sequence of AQP6 contains a tyrosine-based internalization motif (YLLV) beginning at Tyr-10 and a single consensus site for *N*-linked glycosylation at Asn-134. Kidney membranes were incubated with glycosi-

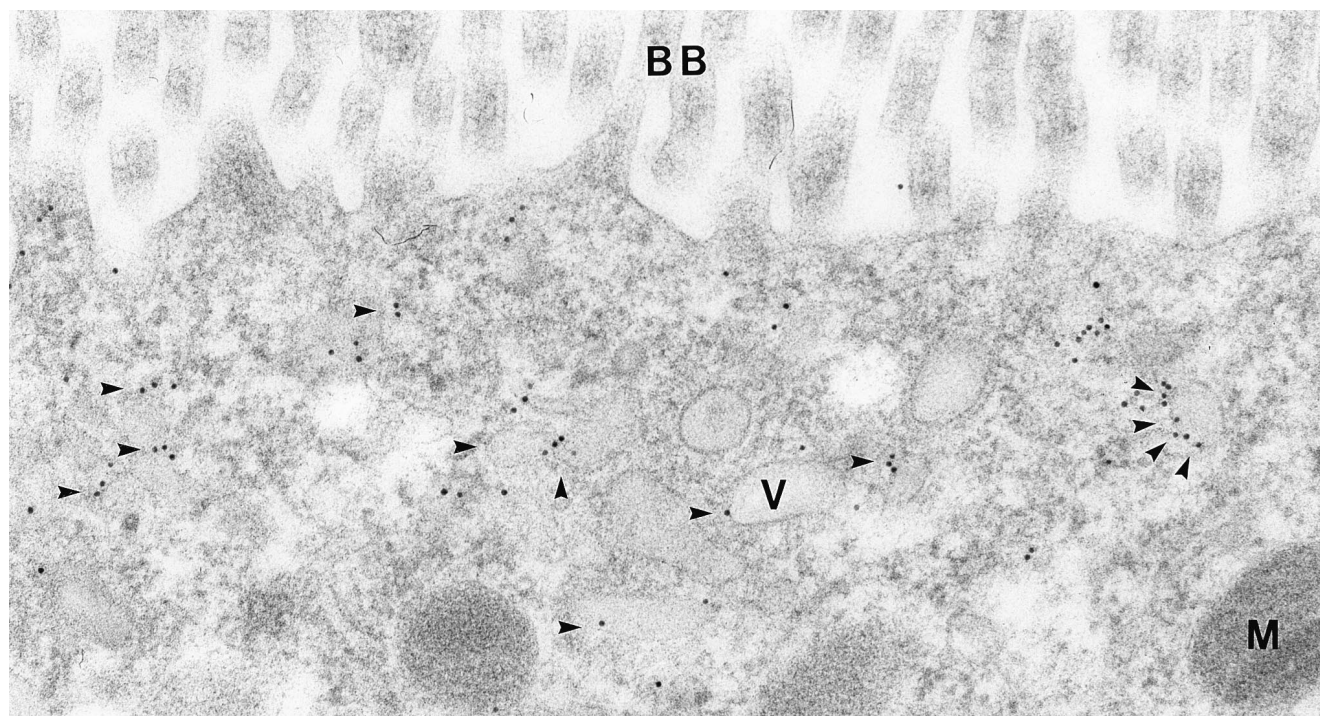


FIG. 4. Immunoelectron microscopy of AQP6 in segment 3 proximal tubule cell. AQP6 labeling of small vesicles (arrowheads) and dense apical tubules in the subapical part of the cell. BB, brush border; M, mitochondria; V, vesicle. Magnification: $\times 85,000$.

dases. Peptide/*N*-glycosidase F is known to cleave all *N*-linked glycans, whereas endoglycosidase Hf is specific for high mannose structures that are found on membrane proteins within intracellular compartments (17). When incubated with either glycosidase, the 30-kDa band in membranes from renal outer medulla was completely digested to a 28-kDa form. Likewise, the less visible 55-kDa band (presumed AQP6 dimer) was reduced by approximately 4 kDa (Fig. 1A, Right). Similar analyses of membranes from renal cortex demonstrated that the 75-kDa band (presumed tetramer) was reduced by approximately 8 kDa (not shown). Thus all contain endoglycosidase Hf-sensitive structures.

To evaluate the possibility that AQP6 may reside within intracellular membrane vesicles, rat renal medulla homogenates were fractionated by sequential ultracentrifugation, with each supernatant used for the next spin and pellets analyzed by immunoblot. As previously reported, AQP1 was found predominantly in the 4,000 and 17,000 $\times g$ fractions (9). In contrast, AQP6 was almost entirely restricted to the 17,000 $\times g$ and 200,000 $\times g$ fractions (Fig. 1B), consistent with residence in an intracellular vesicle compartment as shown for AQP2 (9).

AQP6 in Glomeruli. The regional and segmental distribution of AQP6 was determined with cryostat sections, while the cellular and subcellular sites of expression were established with semithin cryosections or immunoelectron microscopy. In cortex, AQP6 labeling is associated with glomeruli (Fig. 2A and B), where it is present in podocytes; endothelial and mesangial cells exhibited no labeling (Fig. 2B). Immunoelectron microscopy confirmed that AQP6 labeling is almost exclusively confined to intracellular structures in podocyte cell bodies and foot processes; plasma membrane domains exhibited very low labeling (Fig. 3). The intracellular labeling was mainly confined to vesicular structures, and marginal labeling also was associated with multivesicular bodies or lysosomes. Golgi exhibited virtually no labeling. Quantitation of the immunogold labeling of podocytes revealed 1,132 gold particles, with 98.4% associated with intracellular structures and only 1.6% associated with plasma membranes.

AQP6 in Proximal Tubules. AQP6 is also abundantly present in late segment 2 and segment 3 of straight proximal tubules in medullary rays (Fig. 2A), whereas convoluted proximal tubules in the outer cortex exhibited negligible labeling. High-resolution immunocytochemistry confirmed abundant labeling of AQP6 in straight proximal tubule cells (Fig. 2B). The abrupt transition from labeled to unlabeled cells is consistent with distinct segmental localization. Importantly, the labeling is exclusively confined to the subapical domains of the proximal tubule cells. Apical brush border and basolateral plasma membranes were consistently unlabeled (Fig. 2B). Distal convoluted tubules, thick ascending limbs, and vascular structures also were unlabeled.

Immunoelectron microscopy confirmed that AQP6 is predominantly associated with intracellular structures in the subapical domains of proximal tubule cells with no labeling of the brush border (Fig. 4). The labeling is associated with small endocytic vesicles and to a lesser extent to dense apical tubules, whereas endocytic invaginations were only occasionally labeled. Thus, AQP6 is predominantly localized in intracellular vesicles in the proximal tubule cells.

AQP6 in Collecting Duct. Prominent labeling is present within intercalated cells of connecting tubules and cortical collecting ducts (not shown), outer medullary collecting ducts (Fig. 2C–E), and inner medullary collecting ducts in the proximal 25% of inner medulla (Fig. 2E and F). The labeling pattern strongly suggests labeling of type A intercalated cells which was confirmed by immunocytochemistry and immunoelectron microscopy (Figs. 2D and F and 5). The labeled cells are unlikely to correspond to type B intercalated cells, which are restricted to cortical collecting duct, contain much more electron-dense cytoplasm and less prominent microplicae, and lack cytoplasmic tubular profiles. Principal cells were consistently unlabeled (Fig. 2D and F). This distribution was confirmed by immunocytochemistry using anti-AQP2 to label principal cells in parallel semithin cryosections (not shown).

Immunoelectron microscopy of type A intercalated cells revealed that AQP6 is localized in intracellular vesicles and tubulocisternal profiles (Fig. 5), both in the subapical do-

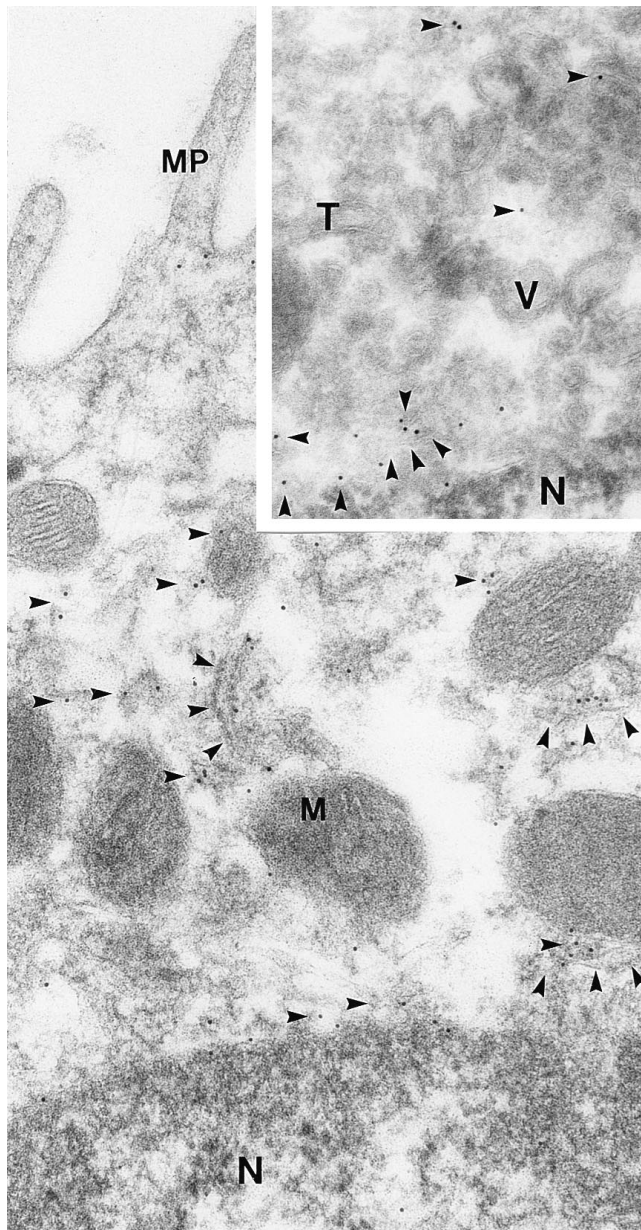


FIG. 5. Immunoelectron microscopy of AQP6 in collecting duct type A intercalated cell from inner stripe of outer medulla. AQP6 labeling of small vesicles and tubulocisternal profiles (arrowheads). (Inset) Ultrathin cryosection of apical part of type A intercalated cell. AQP6 labeling of vesicles and tubulocisternal profiles (arrowheads). MP, microvillae; M, mitochondria; N, nucleus; T, tubulocisternal profiles; V, vesicles. Magnification: $\times 60,000$.

mains and in basolateral domains (Fig. 2 *D* and *F*). No labeling was observed of the apical or basolateral plasma membranes. Immunolabeling of sections from Brattleboro rat kidneys revealed the same labeling pattern. Immunolabeling controls using affinity-purified antibody preabsorbed with excess immunizing peptide (not shown) or with non-immune IgG (Fig. 2 *G* and *H*) produced no labeling. Quantitative analyses of the distribution of 3,695 gold particles over type A intercalated cells revealed that 98.8% were associated with tubulocisternal profiles and vesicles, whereas only 1.2% were associated with plasma membranes. Thus, in podocytes, proximal tubule cells, and type A intercalated cells, AQP6 is almost exclusively localized in intracellular vesicles and is absent or negligibly present in the plasma membrane.

DISCUSSION

Our studies define the sites of expression of AQP6 in rat kidney by using a specific antibody. Like the other AQPs, we found that rat AQP6 has a C-terminal domain that is highly immunogenic in rabbits, in contrast with reports stating that antibodies to synthetic peptides from rat (WCH3) and human homologs (hKID) were nonreactive (12, 13), which may be caused by the frame shift in their sequence (GenBank file L28113). As concluded by others (12, 13), our PCR studies and immunoblots of multiple tissues indicate that AQP6 is predominantly expressed in kidney (not shown). The 75-kDa band in renal cortex does not seem to represent crossreactivity of anti-AQP6 with another protein but probably corresponds to SDS-stable AQP6 tetramers. A similar pattern is found with SDS-stable AqpZ tetramers, which exhibit aberrant mobility during SDS/PAGE (M.J. Borgnia and P.A., unpublished work). Moreover, Northern blots of renal cortex and medulla contain single 2.5-kb signals, suggesting that the 75-kDa and 30-kDa bands of AQP6 are not splice variants (data not shown).

Our biochemical studies indicate that AQP6 resides in an intracellular compartment with a slow transit time. Digestion with endoglycosidase Hf demonstrated a high mannose carbohydrate on each subunit of AQP6 (Fig. 1*A*) and is distinct from the glycosylation pattern of AQP1 in the plasma membrane, which bears a complex glycan on only one subunit per tetramer (22, 23). Appearance of AQP6 in ultracentrifugation fractions containing vesicles (Fig. 1*B*) also predicts residence within the intracellular compartment of renal epithelial cells. Tyrosine-based sorting signals have been implicated in targeting proteins to various intracellular compartments, including endosomes and lysosomes (24). The YLLV motif near its N terminus may be essential for intracellular localization of AQP6 in native tissues.

Immunohistochemical staining and immunogold electron microscopy of kidney revealed that AQP6 is exclusively present in intracellular vesicles that do not overlap with sites where other AQPs reside. No AQPs have previously been identified in glomerular podocytes. Renal proximal tubules contain AQP1 in apical brush border but not subapical vesicles (3), whereas AQP6 has the opposite distribution. Renal collecting duct principal cells contain AQP2 in intracellular vesicles and in the apical plasma membranes (8), whereas AQP6 is located only within intracellular vesicles in the adjacent intercalated cells. Presence of AQP6 in podocytes suggests a possible role in glomerular filtration (25). In proximal tubules and collecting duct, the sites where AQP6 is expressed may coincide with the sites where the CIC-5 chloride channel recently was demonstrated alongside the vacuolar H^+ -ATPase in proximal tubules and type A intercalated cells (26). Specific double-labeling studies will be needed to demonstrate whether the same membrane vesicles contains all three proteins.

Based on the findings reported here, detailed biophysical evaluations of AQP6 are being undertaken. A previous study reported the markedly low water permeability of AQP6 (13). We recently have discovered that when exposed to low pH, the water permeability of AQP6 is rapidly activated and is accompanied by a selective chloride conductance (M.Y., A. Hazama, S.N., W. B. Guggino, and P.A., unpublished work). Moreover, the expression of AQP6 is markedly up-regulated in rats made chronically alkalotic with bicarbonate (M.A.K., M.Y., P.A., and S.N., unpublished work). Its unique tissue distributions and unprecedented transport functions together indicate that AQP6 is unlike the known mammalian AQPs. Our studies predict that AQP6 does not function as a simple conduit for trans-epithelial water absorption or secretion but participates in diverse physiological processes, including acid-base metabolism.

We thank Zhila Nikrozi, Annette Blak Rasmussen, Barbara L. Smith, Mingqi Lu, and Matthew R. T. Hall for assistance. This work was supported by a fellowship from the Human Frontier Science Program (M.Y.), research grants from the Novo Nordic Foundation, the Karen Elise Jensen Foundation, the Danish Medical Research Council, the Biomembrane Research Center at University of Aarhus (S.N.), the National Institutes of Health (M.A.K. and P.A.), and the Cystic Fibrosis Foundation (P.A.). Core oocyte facilities were provided by William B. Guggino, Johns Hopkins School of Medicine, Department of Physiology.

1. Agre, P., Bonhivers, M. & Borgnia, M. J. (1998) *J. Biol. Chem.* **273**, 14659–14662.
2. Nielsen, S., Marples, D., Frøkiær, J., Knepper, M. A. & Agre, P. (1996) *Kidney Int.* **49**, 1718–1723.
3. Nielsen, S., Smith, B. L., Christensen, E. I., Knepper, M. A. & Agre, P. (1993) *J. Cell. Biol.* **120**, 371–383.
4. Denker, B. M., Smith, B. L., Kuhajda, F. P. & Agre, P. (1988) *J. Biol. Chem.* **263**, 15634–15642.
5. Sabolic, I., Valenti, G., Verbavatz, J. M., Van Hoek, A. N., Verkman, A. S., Ausiello, D. A. & Brown, D. (1992) *Am. J. Physiol.* **263**, C1225–C1233.
6. Fushimi, K., Uchida, S., Hara, Y., Hirata, Y., Marumo, F. & Sasaki, S. (1993) *Nature (London)* **361**, 549–552.
7. Deen, P., Verdijk, M., Knoers, N., Wieringa, B., Monnens, L., van Os, C. H. & van Oost, B. A. (1994) *Science* **264**, 92–95.
8. Nielsen, S., Chou, C. L., Marples, D., Christensen, E. I., Kishore, B. K. & Knepper, M. A. (1995) *Proc. Natl. Acad. Sci. USA* **92**, 1013–1017.
9. Ecelbarger, C. A., Terris, J., Frindt, G., Echevarria, M., Marples, D., Nielsen, S. & Knepper, M. A. (1995) *Am. J. Physiol.* **269**, F663–F672.
10. Terris, J., Ecelbarger, C. A., Marples, D., Knepper, M. A. & Nielsen, S. (1995) *Am. J. Physiol.* **269**, F775–F785.
11. Ishibashi, K., Kuwahara, M., Gu, Y., Kageyama, Y., Tohsaka, A., Suzuki, F., Marumo, F. & Sasaki, S. (1997) *J. Biol. Chem.* **272**, 20782–20786.
12. Ma, T. H., Frigeri, A., Skach, W. & Verkman, A. S. (1993) *Biochem. Biophys. Res. Commun.* **197**, 654–659.
13. Ma, T., Yang, B., Kuo, W. & Verkman, A. S. (1996) *Genomics* **35**, 543–550.
14. Agre, P., Sasaki, S. & Chrispeels, M. J. (1993) *Am. J. Physiol.* **265**, F461–F463.
15. Agre, P. (1997) *Biol. Cell* **89**, 255–257.
16. Preston, G. M., Jung, J. S., Guggino, W. B. & Agre, P. (1993) *J. Biol. Chem.* **268**, 17–20.
17. Maley, F., Trimble, R. B., Tarentino, A. L. & Plummer, T. H., Jr. (1989) *Anal. Biochem.* **180**, 195–204.
18. Laemmli, U. K. (1970) *Nature (London)* **227**, 680–685.
19. Nagelhus, E. A., Veruki, M. L., Torp, R., Haug, F. M., Laake, J. H., Nielsen, S., Agre, P. & Ottersen, O. P. (1998) *J. Neurosci.* **18**, 2506–2519.
20. Nielsen, S., Smith, B. L., Christensen, E. I., Agre, P. & Maunsbach, A. B. (1995) *Am. J. Physiol.* **268**, F1023–F1037.
21. Nielsen, S., Nagelhus, E. A., Amiry-Moghaddam, M., Bourque, C., Agre, P. & Ottersen, O. P. (1997) *J. Neurosci.* **17**, 171–180.
22. Smith, B. L., Preston, G. M., Spring, F., Anstee, D. J. & Agre, P. (1994) *J. Clin. Invest.* **94**, 1043–1049.
23. Smith, B. L. & Agre, P. (1991) *J. Biol. Chem.* **266**, 6407–6415.
24. Sandoval, I. V. & Bakke, O. (1994) *Trends Cell Biol.* **4**, 292–297.
25. Andrews, P. (1988) *J. Elect. Microsc. Tech.* **9**, 115–144.
26. Gunther, W., Luchow, A., Cluzeaud, F., Vandewalle, A. & Jentsch, T. J. (1998) *Proc. Natl. Acad. Sci. USA* **95**, 8075–8080.